Chemosensors **2014**, *2*, 207-218; doi:10.3390/chemosensors2030207

OPEN ACCESS

chemosensors

ISSN 2227-9040

www.mdpi.com/journal/chemosensors

Article

Photonic Crystal-Based Sensing and Imaging of Potassium Ions

Christoph Fenzl, Michael Kirchinger, Thomas Hirsch * and Otto S. Wolfbeis

Institute of Analytical Chemistry, Chemo- and Biosensors, University of Regensburg, 93040 Regensburg, Germany; E-Mails: christoph.fenzl@ur.de (C.F.); michael.kirchinger@ur.de (M.K.); otto.wolfbeis@ur.de (O.S.W.)

***** Author to whom correspondence should be addressed; E-Mail: Thomas.hirsch@ur.de; Tel.: +49-941-943-5712; Fax: +49-941-943-4064.

Received: 28 April 2014; in revised form: 4 August 2014 / Accepted: 9 September 2014 / Published: 18 September 2014

Abstract: We report on a method for selective optical sensing and imaging of potassium ions using a sandwich assembly composed of layers of photonic crystals and an ion-selective membrane. This represents a new scheme for sensing ions in that an ionic strength-sensitive photonic crystal hydrogel layer is combined with a K^+-selective membrane. The latter consists of plasticized poly(vinyl chloride) doped with the K^+-selective ion carrier, valinomycin. The film has a red color if immersed into plain water, but is green in 5 mM KCl and purple at KCl concentrations of 100 mM or higher. This 3D photonic crystal sensor responds to K^+ ions in the 1 to 50 mM concentration range (which includes the K^+ concentration range encountered in blood) and shows high selectivity over ammonium and sodium ions. Sensor films were also imaged with a digital camera by exploiting the RGB technique.

Keywords: photonic crystal; chemical sensor; hydrogel; RGB readout; potassium sensing; imaging

---

1. Introduction

Monitoring of potassium ions is of large interest in point-of-care diagnostics on a daily basis, because it is a highly significant parameter for recognizing the occurrence of various kinds of infarction. Moreover, potassium ions govern numerous physiological processes [1], such as the control of blood pressure, nerve signal transmission and muscular strength [2,3]. They regulate the growth of cells [4], affect endothelial function [5] and maintain a concentration gradient (and, thus, the Donnan potential)

between cells and interstitial fluids [6]. A large variability of the concentration of K^+ is indicative of a large number of diseases, for example cardiac arrhythmia or myasthenia [7], alcoholism, diabetes, cancer and others [8]. The determination of potassium concentration [K^+], therefore, is carried out on a large scale in clinical labs. Inside cells, the [K^+] typically is 150 mM, while it is only 4 mM in the extracellular space, for example in serum [9].

[K^+] is routinely analyzed in the clinical lab via ion-selective electrodes [10] or optical sensor membranes [11]. These usually consist of the ionophore, valinomycin [12], incorporated into a (plasticized) solid polymer that permits K^+ ions to be transported into or through the membrane to reach the electrochemical or optical signal transducer, whilst any other ions are excluded. Such sensors suffer, however, from several drawbacks. Electrodes can undergo signal drift and fouling [13], while optical sensors can undergo photobleaching or give weak optical signals or signal changes [14,15].

Chemical sensors based on the use of photonic crystals (PhCs) represent a fairly new class of sensing devices [16]. PhCs consist of periodically arranged structures [17,18] of a dielectric material often placed in a polymer [19]. They reflect light of a certain wavelength that is dependent on: (i) the angle of the incident light; (ii) the distances of beads within the structure; and (iii) the refractive indices of the structure and the surrounding medium [20]. If the initial distance in the PhC is kept constant, for example by placing ordered micro- or nano-particles in a hydrogel matrix, changes in the reflected wavelength will occur if the matrix swells or shrinks [21]. This has been widely used in physical and chemical sensor technology, as this mechanism can be made chemically selective and PhCs possess several advantages, such as low-cost production, ease of up-scaling, ease of readout and being label-free [16].

Numerous PhC-based schemes have been described for use in chemical [19,22] and biological [23–25] sensing. In the field of ion sensing, sensors are known that respond to ionic strength in general [21,26], and, due to the pioneering work of the groups of Asher [27,28], Jana [29] and Watanabe [30], more specifically, to ions of cobalt, copper, nickel, zinc [28], lead [27], mercury [29] and potassium [30]. The sensors are based on the modification of the hydrogel matrix with either enzymes [29] or crown ethers [27,28,30]. Some ions can be discriminated only according to their physical properties, such as radius and charge, or by the inhibitory effect on enzymes displayed by certain heavy metal ions. In order to enable highly-specific sensing in combination with the advantages of PhC technology, such as simple (often visual) readout, the ion recognition must be significantly improved. The sensor for [K^+] described in [30] uses a porous gel that undergoes color changes depending on [K^+], but suffers from the limited selectivity of the crown ether used. Moreover, it was prepared via a templating technique that results in a material of limited temporal and chemical stability. An all-plastic sensor (like practically all other sensors for K^+) is highly desirable, because such sensors can be re-used for quite some time or even operated continuously.

Ionophores are indispensable tools in terms of sensing K^+, and valinomycin is superior to any crown ether [10,31]. We are demonstrating here, by extending the work of Asher *et al.* on PhC sensing technology, a combination of a 3D photonic crystal film with a plasticized PVC membrane containing valinomycin to form a two-layer system. This sensor arrangement is shown to be highly selective for K^+ and to respond to K^+ over a wide concentration range that also covers the level of K^+ encountered in whole blood. We also show that such sensor films can be imaged using either a microscope or a digital camera.

2. Experimental Section

2.1. Materials

Acrylamide, ammonium chloride, 2,2-diethoxyacetophenone, divinylbenzene (DVB), sodium styrenesulfonate (NaSS), poly(vinyl chloride) (PVC), styrene and valinomycin were purchased from Sigma-Aldrich (Taufkirchen, Germany). Dibutyl sebacate, dimethylsulfoxide (DMSO), methanol, *N*,*N*'-methylenebisacrylamide, potassium chloride, potassium nitrate and sodium hydroxide were purchased from Merck (Darmstadt, Germany); and sodium chloride from VWR (Darmstadt, Germany). Sodium bicarbonate was from Ferak (Berlin, Germany) and sodium persulfate ($Na_2S_2O_8$) from Riedel-de Haen (Seelze, Germany). The ion exchange resin (type AG-501 X8) was purchased from Bio-Rad (Munich, Germany), *N*,*N*,*N*',*N*'-tetramethylethylenediamine (TEMED) was from Serva (Heidelberg, Germany), and tetrahydrofuran was from Acros (Geel, Belgium). Styrene was freshly distilled, and divinylbenzene was filtered through basic aluminum oxide before use in order to remove stabilizers.

2.2. Methods

2.2.1. Synthesis of Particles

The negatively-charged crosslinked polystyrene particles were synthesized as described previously by our group [26] with small alterations. Briefly, a mixture of styrene (18.8 g) and divinylbenzene (DVB; 1.2 g) was added to a volume of 152 mL of ultrapure and oxygen-purged water. The mixture was heated to 91 °C under permanent agitation. Next, a solution of 207 mg of sodium styrenesulfonate (NaSS) in 5 mL of water was added. After 3 min, 5 mL of an aqueous initiator solution containing 29 mg of $NaHCO_3$ and 76 mg of $Na_2S_2O_8$ were injected. After another 25 min, 10 mL of water and more monomers/initiator were added in the following order: (I) a mixture of 3.76 g of styrene and 240 mg of DVB; (II) a solution of 641 mg of NaSS in 5 mL of water; and (III) 5 mL of the aqueous initiator solution. After 1 h, the oil bath was removed and the mixture allowed to cool to 25 °C. The suspension was filtered through a double layer of filter paper. For purification, 50 mL of the resulting suspension of nanoparticles were centrifuged for 90 min at a relative centrifugal force (RCF) of 49,000× *g*. The resulting pellets were suspended in 5 mL of water by vortexing and ultrasonic treatment. This procedure was repeated, and the resulting suspension was centrifuged again for 180 min (RCF 49,000× *g*) and redispersed in 5 mL of water. The centrifuged suspension of nanoparticles was diluted with 50 mL of water, and the temperature of the mixture was maintained at 85 °C. After 6 days, the particles were again centrifuged according to the above protocol.

2.2.2. Determination of Particle Size and Zeta Potentials

The particles prepared as described in Section 2.2.1 were dispersed (8 $g \cdot L^{-1}$) in water and vortexed. A 10-µL drop of the suspension was placed on a carbon-coated copper grid. After drying, micrographs were acquired with a transmission electron microscope (TEM; type CM 12; from Philips, Hillsboro, OR, USA). Dynamic light scattering (DLS) measurements were carried out with the same suspensions using a Zetasizer Nano Series instrument (Malvern, Herrenberg, Germany) operated in

backscattering mode at an angle of 173° at 25 °C after temperature equilibration for 60 s. After 20 consecutive measurements, the mean hydrodynamic radius and the polydispersity index (PDI) were extracted from the autocorrelation data.

The electrophoretic mobility of the nanospheres was measured by dispersing them at a concentration of approximately 8 $g \cdot L^{-1}$ in a 10 mM sodium chloride solution after prolonged vortexing and sonication. Around 800 µL of the particle suspension were filled into a folded capillary cell (type DTS1060; from Malvern) and thermostated to 25 °C. Laser Doppler velocimetry with the Zetasizer nano series determined the mean electrophoretic mobility in 400 runs. The Smoluchowski model was used to calculate the ζ-potential of the dispersions.

2.2.3. Preparation of Sensor Films

The hydrogel-based photonic crystal layer was prepared analogously to the protocol described previously [26]. Briefly, acrylamide (50 mg) and *N*,*N*'-methylenediacrylamide (2.5 mg) were dissolved in a suspension of 1 mL of poly(styrene-co-sodium styrenesulfonate) nanoparticles (60 $g \cdot L^{-1}$) in ultrapure water. A solution of 10 µL of 2,2-diethoxyacetophenone in 10 µL of DMSO and 160 mg of ion-exchange resin were added. After intense vortexing and sonication, oxygen was removed by bubbling nitrogen through the vial. The suspension was injected into a polymerization cell consisting of two microscope slides and sidewalls consisting of a Parafilm™ spacer with a thickness of 125 µm. The gel was photopolymerized by UV irradiation at 366 nm (6 W) for 5 h, after which it was fully polymerized, but not yet dry. The film was intensely washed with water. The amino groups were hydrolyzed to form carboxy groups by applying a mixture of 900 µL of 1 M sodium hydroxide and 100 µL of TEMED. After 6 min, the film was thoroughly washed with ultrapure water.

The potassium-selective membrane was prepared as follows: A solution containing 1 g PVC in 10 mL THF and another containing 2 mL of plasticizer (dibutyl sebacate) and 200 µL of valinomycin stock solution (80 $mg \cdot mL^{-1}$ in methanol) were mixed and thoroughly stirred for about 15 min. The mixture was poured in a round glass dish with a diameter of 4 cm, avoiding any air bubbles. After 2 h at room temperature, all of the solvent was evaporated, and a thin membrane formed. It was stored in ultrapure water.

2.2.4. Assembly of the Sensor Films

The partially hydrolyzed polyacrylamide films (with a size of ~1 cm^2) containing polystyrene nanoparticles were placed in the center of a microscope glass slide and wetted with water. The round potassium-selective PVC membrane (diameter 4 cm) was placed tightly on top of the hydrogel by applying gentle physical pressure in order to completely cover the PhC film and to not allow direct access of any compound without passing the PVC membrane.

2.2.5. Measurements of Reflected Light of the Ion-Selective Photonic Crystal

A droplet of 500 µL of solutions of varying salt concentrations was placed on the sensor film assembly. A xenon lamp (0.5 W) was used as an illumination source, and an optical fiber waveguide was fixed at an angle of 90° with respect to the lamp. The fiber was connected to a USB 4000 spectrometer

(Ocean Optics, Ostfildern, Germany). Reflection spectra were recorded with SpectraSuite (Ocean Optics) in the reflectance mode with an integration time of 100 ms per spectrum. All measurements were performed under ambient conditions at room temperature.

2.2.6. Microscope Imaging Technique for Sensor Films

The PhC sensor film was placed under a microscope (Leica DMRE, Leica, Wetzlar, Germany) and viewed with 50-fold enlargement. The film was immersed in aqueous solutions of varying salt concentrations, and a picture was acquired immediately thereafter. The exposure time was set to 10 ms, saturation to 0.85 and the gamma correction of the luminance of the camera to 1.3. These settings were kept constant so that all images were acquired under identical conditions and are comparable. Pictures were separated into a blue, green and red channel (RGB). Generally, the intensity of each respective channel is between 0 and 255. Data evaluation was performed with ImageJ freeware.

3. Results and Discussion

3.1. Choice of Materials and Sensor Layout

As shown in previous work [26], 3D PhCs can be prepared in a very efficient way via controlled arrangement of periodic dielectric, highly charged, monodisperse polystyrene spheres. Styrene can easily be polymerized and crosslinked, and its size and low polydispersity can be well adjusted by surfactants. Sulfonate groups are introduced by using styrenesulfonate as a secondary monomer. The fraction of reagents and the reaction conditions are the result of an optimization of the concentrations of cross-linker and initiator and of polymerization time. The concentration, surface charge and size of the particles are exerting several effects. Surface charges and particle diameters that are too small will lead to particle-particle distances where diffraction occurs in the UV rather than in the visible. If, on the other side, the surface charge and spheres are too large, the opposite effect will take place, and the diffracted light will come to lie in the near IR, so that films will appear colorless to the eye. Generally speaking, the particle number densities must be in the proper range for light diffraction in the visible to occur.

Polyacrylamide (PAM) is a good choice in terms of matrix (host) material for the polystyrene particles. It is well permeated by ions, and all of the components are water-soluble and transparent, so the structural colors of the photonic crystal dispersions can be recorded without the optical influence of the hydrogel. In order to render the film sensitive to ionic strength, the amido groups of PAM are (partially) hydrolyzed to form (anionic) carboxylate groups. We have shown in an earlier study [26] that the reflected wavelength of such generated sensor films is stable between 4 and 60 °C.

The second film is composed of a plasticized PVC membrane and doped with the cyclodepsipeptide, valinomycin, the most common and best ionophore for K^+, in the same fashion as reported for K^+-selective electrodes [10,31]. Valinomycin shows a ~10^5-fold selectivity for K^+ over Na^+ and is very stable. The combination of a valinomycin-modified plasticized PVC membrane with a PhC system sensitive to ionic strength resulted in a new sensor for the determination of potassium ions. A schematic of the sensor layout is shown in Figure 1.

Figure 1. Cross-section of the photonic crystal (PhC)-based sensor for potassium ions. Bottom layer: microscope glass slide (width 2.5 cm). Center layer: a partially hydrolyzed wet polyacrylamide film (size ~1 cm^2) containing polystyrene nanoparticles. Top layer: potassium-selective plasticized PVC membrane (diameter 4 cm). The sample containing K^+ ions is placed on the top layer.

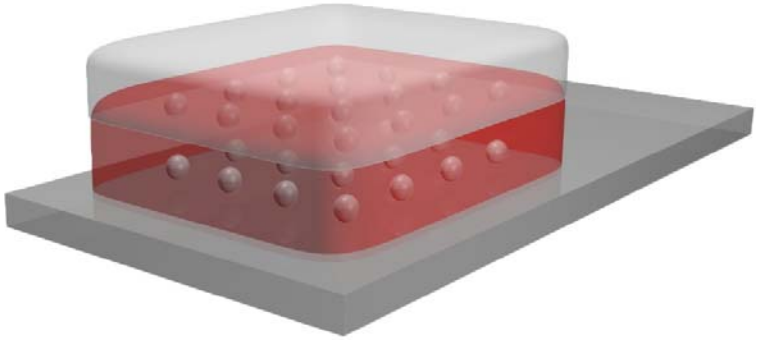

3.2. Characterization of Polystyrene Nanoparticles

TEM and DLS were used to determine the diameter of the polystyrene nanoparticles. As expected, the hydrodynamic radius (determined by DLS) is larger than the physical radius (determined by TEM), as the high surface charge causes an extended hydration shell, which makes the particle appear larger in light scattering experiments. The mean diameter as calculated by evaluating 61 particles in the TEM image is 84 ± 8 nm (Figure 2), while DLS measurements showed a hydrodynamic diameter of 92 nm with a polydispersity index of 0.14. A zeta potential of −51.6 mV was calculated from the electrophoretic mobility data and proves the expected highly negative surface charge due to the presence of sulfonate groups in the polymer.

Figure 2. TEM image (**left**) and corresponding size distribution (**right**) of monodisperse nanoparticles consisting of styrene, divinylbenzene and sodium styrene sulfonate.

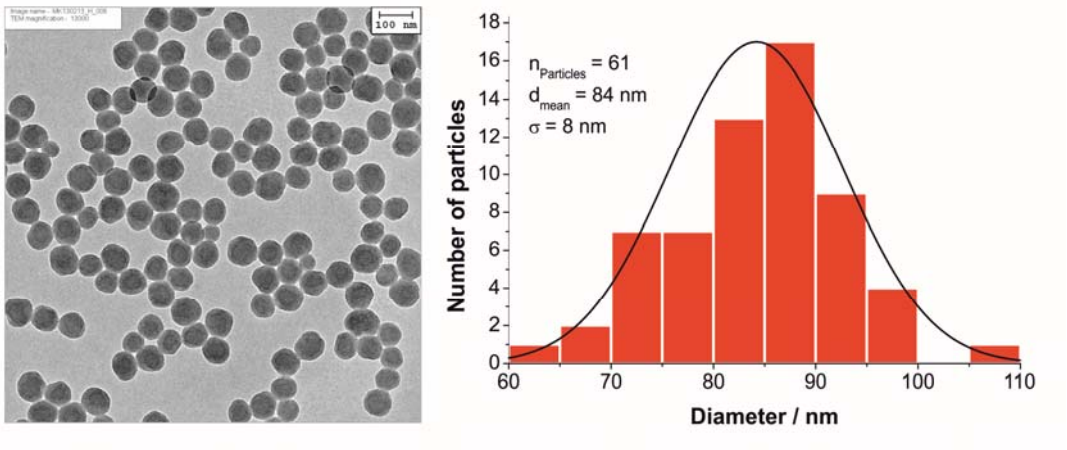

For the sensor application presented herein, it is desirable that the nanoparticle dispersions reflect visible light, so as to enable a visual readout. We therefore tuned the size and surface charge of the particles, such that the films display a strong violet reflectance. As proven in earlier studies [26], the particles also show a long-term stability of better than one year.

3.3. Sensing Performance

In order to quantify the potassium sensing properties of this novel combination of materials, the device was immersed into aqueous solutions containing different salts in varying concentrations, but at a constant pH value (Figure 3). Ammonium chloride, potassium chloride, potassium nitrate and sodium chloride were tested in concentrations between 10 µM and 0.5 M. In order to determine the sensitivity of the photonic crystal film alone, KCl solutions were also applied to a PAM film without valinomycin/PVC membrane coverage. The presence of K^+ ions induces a color change at K^+ concentrations between 0.1 mM and 0.1 M. The response is virtually instantaneous (<10 s), and the effects are fully reversible without the need for adding any other reagents. In comparison to an ionic strength sensor without PVC film [26], response times are marginally longer (~2–5 s), due to the ion-selective membrane coverage. The logarithmic plot is linear in the concentration range between 1 and 50 mM, and the slope is 53 nm per one log order of $[K^+]$. This obviously also covers the typical concentration of K^+ in serum (~4 mM). In addition, the sensor is very selective in that monovalent cations of approximately the same size (ammonium and sodium) do not cause a signal change over the whole concentration range (Figure 3). This also confirms that the PVC membrane prevents the direct contact of the analyte with the PhC film. The corresponding anion appears not to have an effect, since KCl and KNO_3 give the same response.

Figure 3. The effect of the salt concentration on the wavelength of the reflected light of colloidal PhCs in a hydrolyzed PAM hydrogel covered with a K^+-selective membrane. The film was immersed into solutions of KCl, KNO_3, NaCl and NH_4Cl of varying concentrations. Each data point represents the average of five measurements; the error bars display the respective standard deviations.

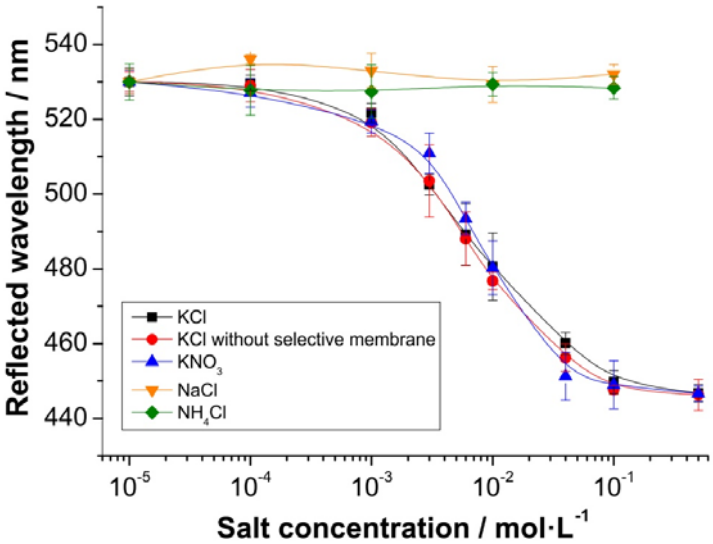

It is useful to have a look at the PhC-based sensor for K^+ described by Saito *et al.* [30]. It is composed of a single-layer consisting of poly(N-isopropylacrylamide) (PNIPAM) modified with a crown ether. The maximum of the reflected wavelength shifts from 500 to 700 nm if $[K^+]$ is increased from 0 and 40 mM, and its lower limit of detection is rather high (5 mM). By comparison, the sensor film presented here undergoes a smaller spectral shift (from 530 to 440 nm), but has a much higher dynamic range

(from 0.1 to 100 mM). In addition, the PNIPAM-based sensor does not respond linearly, and solutions containing ammonium cations (which are known to bind to certain crown ethers) have not been examined [30]. Finally, the maximum wavelength of reflection of PNIPAM is known to be highly temperature-dependent. We therefore believe that our system has distinct advantages.

3.4. Imaging Potassium Concentrations

The good correlation between the color of the sensor film and the concentration of K^+ prompted us to study whether such films may be read out ("imaged") using a digital camera mounted on a microscope. This method has been proven to be a viable, rapid and convenient approach to quantify the changes in color or fluorescence as they occur in sensor films designed to detect and image, for example, salinity [26], oxygen and pH values *in vivo* [32] or air pressure and temperature [33]. Others have used smart phones that can serve the same purpose ([34] and the references cited therein). The pictures of our new sensor films exposed to various concentration of K^+ were acquired with a digital camera and a microscope and are shown in Figure 4.

Figure 4. Microscope images (50-fold enlargement) of the photonic crystal film immersed into water solutions of KCl in varying concentrations.

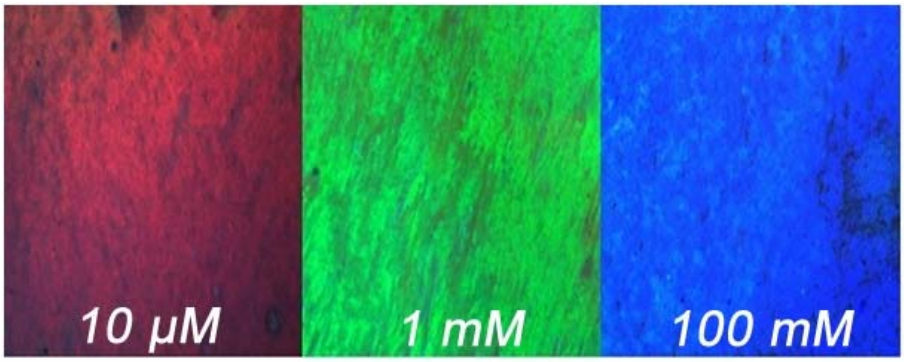

The RGB data sets of the digital pictures were then separated into the three-color channels (red, green and blue; RGB) of which any digital picture is composed. Subsequent mathematical processing allows analytical evaluation of the potassium ion content of aqueous solutions (Figure 5). The normalized values were obtained from the absolute individual RGB intensity by division through the maximum value of the average intensity of the respective channel ($I_{rel} = I/I_{max(av)}$). The standard deviations of the blue and the green channel obviously are too high to allow for a precise calculation of $[K^+]$, but an evaluation of the red channel reveals an almost linear decrease (by 80%) in intensity on going from 10 µM to 10 mM potassium concentrations. Although the errors seem very high in general, these standard deviations symbolize the batch variation from sensor to sensor, with these resulting from measurements with five different films prepared by the same protocol. The errors obtained from a single film used for consecutive measurements are negligibly small. Then, the blue channel can also be used for content analysis, as its intensity rises 62% when the concentration of potassium ions increases from 1 to 10 µM.

Figure 5. Relative intensities of the blue, green and red channel of a digital picture of a sensor layer immersed in solutions of KCl in varying concentrations. Pictures were acquired with a camera mounted on a microscope with 50-fold magnification. Each data point presents the average of five measurements. The error bars give standard deviations.

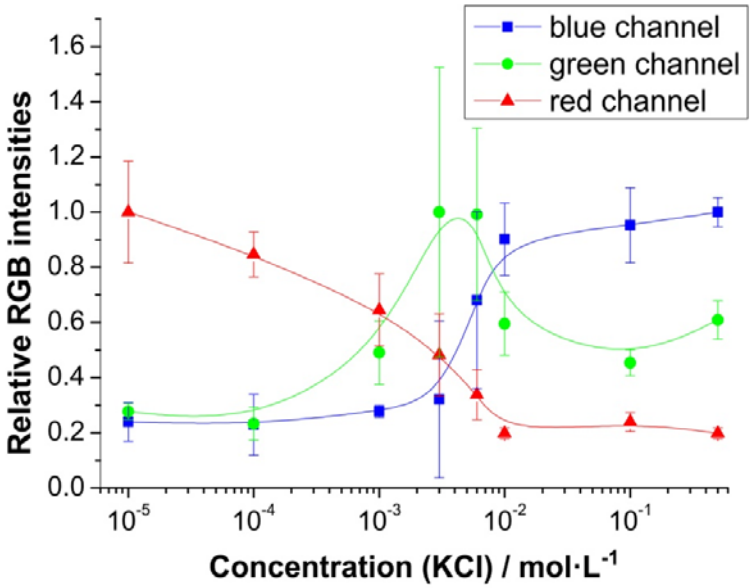

4. Conclusions

We are presenting a two-layer approach towards optical sensing of K^+ using photonic crystal sensor technology. It is capable of detecting K^+ in the 0.1 to 100 mM concentration range over which a visually and instrumentally detectable wavelength shift of 90 nm is induced. This range also covers the one found in human blood. The sensor films can be fairly easily prepared from affordable materials. Aside from bare-eye (visual) detection, the films can be read out by reflectometry in the visible part of the spectrum. In addition, they can be imaged using a digital camera. An increase in [K^+] from 10 µM to 10 mM causes the intensity of the red channel of the reflected light to decrease by 80%. The sensor is highly selective in that other alkali and earth alkaline ions remain inert. Other features include fast response, lack of photobleaching, full reversibility on exposure to plain water (*i.e.*, without adding another reagent) and inertness to changes in stability, as shown in previous work [26].

Given these features, we presume that this sensor is a viable tool for both single-shot and continuous sensing of [K^+] at physiological concentrations. Conceivably, the sensor is produced in the form of a test stripe for on-site (near-patient) visual readout. This proof of principle of sensing ions using a PhC-based two-layer technology is exploiting the fact that the photonic crystals placed in a hydrogel layer can be made sensitive to ionic strength. It is combined with ion-selective membrane technology in order to make the sensor specific for an ion. Given the fact that a large variety of ionophores is known, we predict that this sensing scheme can be extended to a number of other ions and even to sensor arrays for multiple ion sensing.

Acknowledgments

Stefan Wilhelm is thanked for acquiring many of the TEM pictures.

Author Contributions

C.F. and M.K. synthesized and characterized the polystyrene nanoparticles, fabricated the PhC film and collected the data. C.F. and T.H. advised the experimental design and were responsible for data analysis. C.F. wrote the manuscript. T.H. and O.S.W. supervised the overall experimental design and writing. All authors discussed the results and commented on the manuscript.

Conflicts of Interest

The authors declare no conflict of interest.

References

1. Sun, H.; Li, X.; Li, Y.; Fan, L.; Kraatz, H.-B. A novel colorimetric potassium sensor based on the substitution of lead from G-quadruplex. *Analyst* **2013**, *138*, 856–862.
2. He, H.; Mortellaro, M.A.; Leiner, M.J.P.; Fraatz, R.J.; Tusa, J.K. A Fluorescent Sensor with High Selectivity and Sensitivity for Potassium in Water. *J. Am. Chem. Soc.* **2003**, *125*, 1468–1469.
3. Teresa, M.; Gomes, S.R.; Tavares, K.S.; Oliveira, J.A.B.P. The quantification of potassium using a quartz crystal microbalance. *Analyst* **2000**, *125*, 1983–1986.
4. Niemeyer, M.I.; Cid, L.P.; Barros, L.F.; Sepúlveda, F.V. Modulation of the Two-Pore Domain Acid-sensitive K^+ Channel TASK-2 (KCNK5) by Changes in Cell Volume. *J. Biol. Chem.* **2001**, *276*, 43166–43174.
5. Young, D.B.; Ma, G. Vascular protective effects of potassium. *Semin. Nephrol.* **1999**, *19*, 477–486.
6. Shieh, C.C.; Coghlan, M.; Sullivan, J.P.; Gopalakrishnan, M. Potassium Channels: Molecular Defects, Diseases, and Therapeutic Opportunities. *Pharmacol. Rev.* **2000**, *52*, 557–594.
7. Sanguinetti, M.C.; Tristani-Firouzi, M. hERG potassium channels and cardiac arrhythmia. *Nature* **2006**, *440*, 463–469.
8. Zhou, X.; Su, F.; Tian, Y.; Youngbull, C.; Johnson, R.H.; Meldrum, D.R. A New Highly Selective Fluorescent K^+ Sensor. *J. Am. Chem. Soc.* **2011**, *133*, 18530–18533.
9. Soldin, S.J.; Brugnara, C.; Wong, E.C. *Pediatric Reference Ranges*; American Association for Clinical Chemistry: Washington, DC, USA, 2003.
10. Qin, W.; Zwickl, T.; Pretsch, E. Improved Detection Limits and Unbiased Selectivity Coefficients Obtained by Using Ion-Exchange Resins in the Inner Reference Solution of Ion-Selective Polymeric Membrane Electrodes. *Anal. Chem.* **2000**, *72*, 3236–3240.
11. Krause, C.; Werner, T.; Huber, C.; Wolfbeis, O.S.; Leiner, M.J.P. pH-Insensitive Ion Selective Optode: A Coextraction-Based Sensor for Potassium Ions. *Anal. Chem.* **1999**, *71*, 1544–1548.
12. Crespo, G.A.; Bakker, E. Ionophore-based ion optodes without a reference ion: Electrogenerated chemiluminescence for potentiometric sensors. *Analyst* **2012**, *137*, 4988–4994.
13. He, H.; Li, H.; Mohr, G.; Kovacs, B.; Werner, T.; Wolfbeis, O.S. Novel type of ion-selective fluorosensor based on the inner filter effect: An optrode for potassium. *Anal. Chem.* **1993**, *65*, 123–127.
14. Bühlmann, P.; Pretsch, E.; Bakker, E. Carrier-Based Ion-Selective Electrodes and Bulk Optodes. 2. Ionophores for Potentiometric and Optical Sensors. *Chem. Rev.* **1998**, *98*, 1593–1688.

15. Krause, C.; Werner, T.; Huber, C.; Wolfbeis, O.S. Emulsion-Based Fluorosensors for Potassium Featuring Improved Stability and Signal Change. *Anal. Chem.* **1999**, *71*, 5304–5308.
16. Fenzl, C.; Hirsch, T.; Wolfbeis, O.S. Photonic Crystals for Chemical Sensing and Biosensing. *Angew. Chem. Int. Ed.* **2014**, *53*, 3318–3335.
17. Von Freymann, G.; Kitaev, V.; Lotsch, B.V.; Ozin, G.A. Bottom-up assembly of photonic crystals. *Chem. Soc. Rev.* **2013**, *42*, 2528–2554.
18. Pal, S.; Fauchet, P.M.; Miller, B.L. 1-D and 2-D Photonic Crystals as Optical Methods for Amplifying Biomolecular Recognition. *Anal. Chem.* **2012**, *84*, 8900–8908.
19. Fenzl, C.; Hirsch, T.; Wolfbeis, O. Photonic Crystal Based Sensor for Organic Solvents and for Solvent-Water Mixtures. *Sensors* **2012**, *12*, 16954–16963.
20. Joannopoulos, J.D.; Johnson, S.G.; Winn, J.N.; Meade, R.D. *Photonic Crystals: Molding the Flow of Light (Second Edition)*; Princeton University Press: Princeton, NJ, USA, 2008.
21. Lee, K.; Asher, S.A. Photonic Crystal Chemical Sensors: pH and Ionic Strength. *J. Am. Chem. Soc.* **2000**, *122*, 9534–9537.
22. Zhang, J.T.; Smith, N.; Asher, S.A. Two-Dimensional Photonic Crystal Surfactant Detection. *Anal. Chem.* **2012**, *84*, 6416–6420.
23. Han, J.H.; Kim, H.J.; Sudheendra, L.; Gee, S.J.; Hammock, B.D.; Kennedy, I.M. Photonic Crystal Lab-On-a-Chip for Detecting Staphylococcal Enterotoxin B at Low Attomolar Concentration. *Anal. Chem.* **2013**, *85*, 3104–3109.
24. Deng, G.; Xu, K.; Sun, Y.; Chen, Y.; Zheng, T.; Li, J. High Sensitive Immunoassay for Multiplex Mycotoxin Detection with Photonic Crystal Microsphere Suspension Array. *Anal. Chem.* **2013**, *85*, 2833–2840.
25. Huang, C.S.; Chaudhery, V.; Pokhriyal, A.; George, S.; Polans, J.; Lu, M.; Tan, R.; Zangar, R.C.; Cunningham, B.T. Multiplexed Cancer Biomarker Detection Using Quartz-Based Photonic Crystal Surfaces. *Anal. Chem.* **2012**, *84*, 1126–1133.
26. Fenzl, C.; Wilhelm, S.; Hirsch, T.; Wolfbeis, O.S. Optical Sensing of the Ionic Strength Using Photonic Crystals in a Hydrogel Matrix. *ACS Appl. Mater. Interfaces* **2013**, *5*, 173–178.
27. Asher, S.A.; Sharma, A.C.; Goponenko, A.V.; Ward, M.M. Photonic Crystal Aqueous Metal Cation Sensing Materials. *Anal. Chem.* **2003**, *75*, 1676–1683.
28. Reese, C.E.; Asher, S.A. Photonic Crystal Optrode Sensor for Detection of Pb^{2+} in High Ionic Strength Environments. *Anal. Chem.* **2003**, *75*, 3915–3918.
29. Arunbabu, D.; Sannigrahi, A.; Jana, T. Photonic crystal hydrogel material for the sensing of toxic mercury ions (Hg^{2+}) in water. *Soft Matter* **2011**, *7*, 2592–2599.
30. Saito, H.; Takeoka, Y.; Watanabe, M. Simple and precision design of porous gel as a visible indicator for ionic species and concentration. *Chem. Commun.* **2003**, 2126–2127.
31. Bakker, E.; Pretsch, E. Modern Potentiometry. *Angew. Chem. Int. Ed.* **2007**, *46*, 5660–5668.
32. Meier, R.J.; Schreml, S.; Wang, X.; Landthaler, M.; Babilas, P.; Wolfbeis, O.S. Simultaneous Photographing of Oxygen and pH In-Vivo Using Sensor Films. *Angew. Chem. Int. Ed.* **2011**, *50*, 10893–10896.

33. Fischer, L.H.; Karakus, C.; Meier, R.J.; Risch, N.; Wolfbeis, O.S.; Holder, E.; Schäferling, M. Referenced Dual Pressure- and Temperature-Sensitive Paint for Digital Color Camera Read Out. *Chem. Eur. J.* **2012**, *18*, 15706–15713.
34. Rajendran, V.K.; Bakthavathsalam, P.; Ali, B.M.J. Smartphone based bacterial detection using biofunctionalized fluorescent nanoparticles. *Microchim. Acta* **2014**, 1–7.